Eur Spine J (2005) 14: 346–355
DOI 10.1007/s00586-004-0758-5

ORIGINAL ARTICLE

P. C. Ivancic
Manohar M. Panjabi
S. Ito
P. A. Cripton
J. L. Wang

Biofidelic whole cervical spine model with muscle force replication for whiplash simulation

Received: 21 July 2003
Revised: 7 January 2004
Accepted: 7 May 2004
Published online: 12 October 2004

P. C. Ivancic · M. M. Panjabi (✉)
Biomechanics Research Laboratory,
Department of Orthopaedics and
Rehabilitation, Yale University School
of Medicine, 333 Cedar St.,
P.O. Box 208071, New Haven,
Connecticut 06520-8071, USA
E-mail: manohar.panjabi@yale.edu
Tel.: +1-203-7852812
Fax: +1-203-7857069

S. Ito
Department of Orthopaedic Surgery,
St. Marianna University School
of Medicine, Kanagawa, Japan

P. A. Cripton
Department of Mechanical Engineering,
University of British Columbia,
Vancouver, British Columbia, Canada

J. L. Wang
Institute of Biomedical Engineering,
National Taiwan University,
Taipei, Taiwan

Abstract Whiplash has been simulated using volunteers, whole cadavers, mathematical models, anthropometric test dummies, and whole cervical spines. Many previous in vitro whiplash models lack dynamic biofidelity. The goals of this study were to (1) develop a new dynamic whole cervical spine whiplash model that will incorporate anterior, lateral and posterior muscle force replication, (2) evaluate its performance experimentally and (3) compare the results with in vivo data. To evaluate the new model, rear-impact whiplash simulations were performed using the incremental trauma approach at maximum measured T1 horizontal accelerations of 3.6 g, 4.7 g, 6.6 g, and 7.9 g. The kinematic response of the new model, e.g., peak head–T1 extension and peak intervertebral rotations, were compared with the corresponding in vivo data. The average peak head–T1 extension was within the in vivo corridor during the 3.6 g whiplash simulation (9.1 kph delta V). The peak in vivo intervertebral rotations obtained during a 4.6 g whiplash simulation of a young volunteer were within, or only marginally in excess of, the 95% confidence limits of the average peak intervertebral rotations measured during the 4.7 g whiplash simulation of the present study. Thus, the new whole cervical spine model with muscle force replication produced biofidelic dynamic responses to simulated whiplash. The new model is capable of generating important biomechanical data that may help improve our understanding of whiplash injuries and injury mechanisms.

Keywords Whiplash · Biomechanics · Muscle force replication

Introduction

Cervical spine soft-tissue injuries that occur during automobile collisions can have potentially disabling and life-altering effects [1, 69, 75, 81]. Although the injuries are often difficult to detect, they include ligamentous and anterior annulus tears, facet-joint hemarthroses, articular cartilage damage and synovial-fold displacement [11, 18, 31, 80].

A variety of modeling strategies have been investigated to further understand the whiplash injury mechanisms, including human volunteer tests [10, 34, 37, 47, 48, 49, 55, 71, 78], mathematical models [12, 15, 16, 19, 20, 29, 39, 52, 87], anthropometric test dummies [8, 17, 25, 40, 41, 71, 76, 77], whole cadavers [22, 23, 24, 25, 28, 45, 50, 89] and isolated, whole cervical spine (WCS) specimens [13, 14, 26, 59, 60, 62, 74, 90]. The in vivo studies have provided insight into

head and neck kinematics [33, 34, 47, 48, 49, 55, 71] and the electromyographic activity of the neck musculature [10, 37, 46, 78]. However, by necessity, the in vivo studies apply impacts below the injury threshold. Mathematical models for whiplash simulation of the cervical spine include multibody lumped-parameter [19, 20, 29, 39] and finite-element method models [12, 15, 52, 87]. While mathematical models can incorporate detailed spinal anatomy, including muscles, the output data are highly dependent upon the accuracy of the input data, such as the dynamic mechanical properties of the soft tissues (ligaments and discs) and the muscle activation patterns. Currently, such input data measured at high loading rates are available only in limited form [61, 88]. The mathematical models are typically validated by selecting and simulating an in vivo experiment from the literature, thus limiting the validation to the particular sub-injury in vivo experiment selected [57, 58]. Rear-impact simulations have been performed using anthropometric test dummies seated in automobiles or sleds [8, 17, 25, 40, 41, 71, 76, 77]. High-speed crash simulations provide information useful for identifying the deficiencies in automobile crashworthiness and occupant-protection systems. However, the kinematic response of dummy necks during low-speed collisions lacks biofidelity [17, 25, 39, 40, 71]. Whiplash simulations of whole cadavers seated within sleds have been conducted to model the response of an unwarned occupant [22, 23, 24, 25, 28, 45, 50, 89]. Some limitations of whole-cadaver tests include the inability to quantify soft-tissue injury, inconsistencies in neutral posture alignment and lack of appropriate validation with in vivo data. Several in vivo studies of volunteers have found that muscle tension did not alter head–neck kinematics if the muscles were relaxed prior to the collision, thus providing rationale for the use of cadaveric material for whiplash simulation [55, 78].

Whiplash simulation of WCS specimens [13, 14, 26, 59, 60, 62, 74, 90] mounted on mini-sleds has led to a further understanding of cervical spine injury mechanisms, at significantly lower costs than the whole cadaver experiments [26, 59, 60, 62]. Although the WCS model has shown its many advantages, e.g., injury quantification via pre- and post-whiplash-flexibility testing, it is not biofidelic with respect to spinal loads and postural stability. Recently, several in vitro lumbar [65, 67, 68, 70, 86] and cervical spine [7, 35, 63, 66] quasi-static models have been presented that included various muscle force simulation techniques. The goals of the current study were to develop a new dynamic WCS model for whiplash simulation that will incorporate muscle force replication, and then to evaluate its performance experimentally and compare the results with the available in vivo data.

Materials and methods

The specimens and preparation of the WCS model

A WCS model is constructed from a fresh-frozen whole cervical spine specimen consisting of the occiput (C0) to the T1 vertebra. Six specimens were prepared—four male and two female donors, with an average age of 70.8 years (range, 52–84 years). To prepare a specimen, all non-osteoligamentous soft tissues were carefully dissected, and C0 and T1 were set in two parallel, horizontal resin mounts (Fibre Glass-Evercoat, Cincinnati, OH, USA). A pair of anchoring bolts was embedded into the occipital mount for attachment of the surrogate head. The specimen was mounted such that a line from the tip of the dens to the lowest point on the posterior occiput was parallel to the occipital mount, and the T1 vertebra was tilted anteriorly by 24° [9]. To attach motion-measuring flags, headless wood screws aligned sagittally were drilled into each vertebral body (C2 through C7) and the left lateral mass of C1. The flags, consisting of lightweight, hollow brass tubes, were rigidly fixed onto the vertebral screws.

The WCS model with muscle force replication

In order to enhance the in vivo-like response (i.e., dynamic biofidelity) of the WCS model, a new muscle force replication (MFR) system was developed [30, 64] (Fig. 1 and Table 1). The MFR system consisted of anterior, posterior and lateral cables attached at one end to either the occiput or the cervical vertebra, and to tension springs anchored to the base, at the other end. All MFR springs had a stiffness coefficient of 4.0 N/mm. Customized load cells, constructed of 3.0 mm-thick aluminum C-channels and mounted between the springs and base, were developed to monitor the MFR forces.

To prepare a specimen for the application of the anterior MFR, two headless wood screws were drilled into the anterior aspect of C4 for attachment of posts to serve as guides for the anterior MFR cables. The posts consisted of 3.5 cm-long hollow brass tubes secured to the headless screws and anterior hooks, through which the MFR cables passed. To apply the posterior MFR, wire loops were attached to each spinous process. For the lateral MFR, stainless steel lateral guide rods (3.0 mm diameter) were inserted in the frontal plane into the vertebral bodies of C2 through C7. The lateral rods at C3 through C7 were positioned at the approximate centers of rotation of C2–C3 through C6–C7, respectively. Since C1 does not have a vertebral body, no rod was inserted at this level. The lateral rods were inserted under fluoroscopic control to confirm proper placement and a laterally directed path.

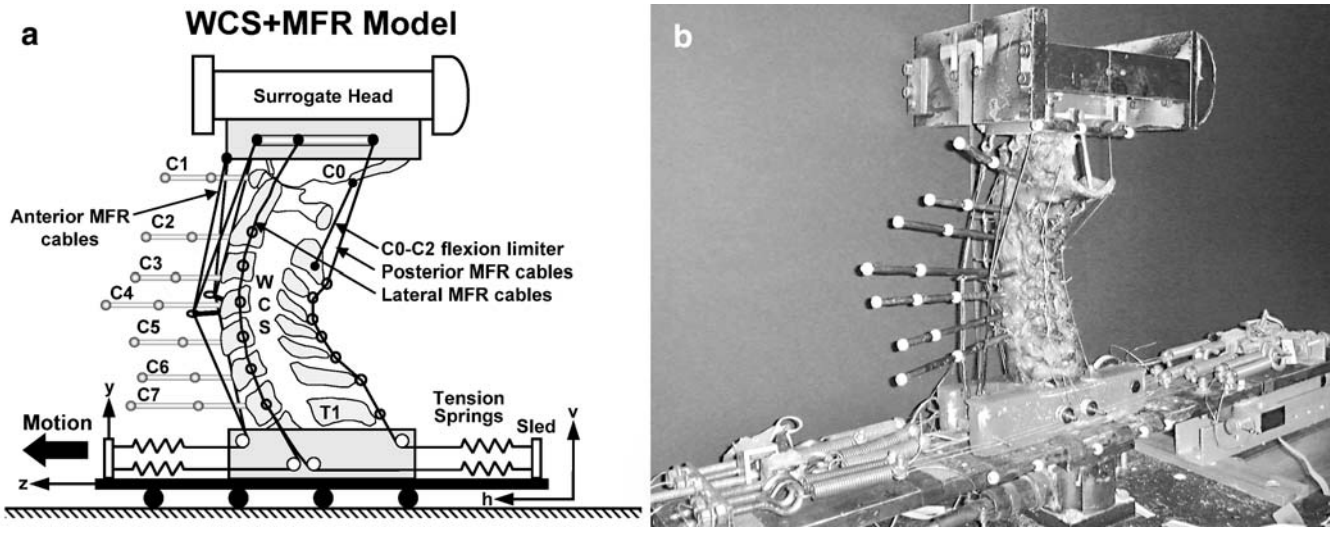

Fig. 1 **a** The WCS + MFR model: whole cervical spine (WCS) with muscle force replication (MFR). Anterior and posterior MFR cables originated from the occipital mount and passed along the anterior and posterior aspects of the WCS, respectively. The lateral MFR cables originated at C0, C2, C4 and C6. The other ends of all cables were attached to the sled via tension springs. The C0–C2 flexion limiter was a wire connecting the posterior base of the occiput to the C2 spinous process. Coordinate system h–v was fixed to the ground and z–y was fixed to the sled; **b** photograph of the WCS + MFR model ready for whiplash simulation

The anterior and posterior MFR Two anterior cables, each consisting of two strands, were anchored to the occipital mount, with two strands attached bilaterally and two strands attached sagittally. The cables each ran through a separate post at C4, through pulleys within the T1 mount (4 cm anterior to the anterior aspect of the T1 vertebral body), and were each connected to a separate spring. The pre-load in each anterior cable was 15 N. The purpose of the C4 posts was to increase the resisting moment during head extension. The posterior MFR cable, consisting of two strands connected bilaterally to the occipital mount, ran sagittally through the wire loops attached to the spinous processes and through a pulley within the T1 mount. The pre-load in the posterior cable was 30 N. The cables (1,200 N load capacity, 1.6 mm diameter, part No. Y-MCX-64, Small Parts, Miami Lakes, FL, USA) were nylon-coated to decrease friction.

Table 1 Muscle force replication parameters including the number of cables (*n*), spring stiffness, and cable pre-loads for the model in the neutral posture

n	Anterior 2	Posterior 1	Lateral 8
Spring stiffness (N/mm)	4	4	4
Cable pre-load (N)	15	30	30

The lateral MFR Bilateral MFR cables originated from C0, C2, C4 and C6, passed around the guide rods, alternately anteriorly and posteriorly, and through pulleys at the T1 mount. The eight cables were each connected to a separate spring, pre-loaded to 30 N. These cables were monofilament nylon (222 N load capacity, 0.7 mm diameter, Omniflex monofilament cable, Shakespeare, Columbia, SC, USA).

The C0–C2 flexion limiter A C0–C2 flexion limiter was used to model the effect of chin-sternum contact on flexion of C0–C1 and C1–C2. To simulate this, a nylon-coated steel cable (180 N load capacity, 0.6 mm diameter, part No. Y-MCX-24, Small Parts, Miami Lakes, FL) was secured to the occipital mount and to the C2 spinous process. The cable length was adjusted so that the total physiological sagittal rotation (flexion plus extension) between the occiput and C2 was approximately 30°, which was within the in vivo range [21, 38, 56].

Intervertebral compressive pre-loads The resulting intervertebral compressive pre-loads in the neutral posture due to all MFR cables were (Table 1): 120 N (C0–C1, C1–C2); 180 N (C2–C3, C3–C4); 240 N (C4–C5, C5–C6); and 300 N (C6–C7, C7–T1). These load magnitudes are in good agreement with the in vivo spinal loads estimated to range between 53 and 1,175 N, depending on the posture [27, 51].

Surrogate head A surrogate head with 3.3 kg mass and a 0.016 kg m^2 sagittal-plane moment of inertia was fixed to the occipital mount at the appropriate height. While the head mass measured from cadavers ranged between 2.8 and 5.8 kg [6, 83], we chose the 3.3 kg mass for the following reason. We assumed that the donors (average age 70.8 years) of our specimens most likely expired

after prolonged illness and bed rest. During this time, there would have been, in addition to the normal age-related decreases in bone mass, density and strength, further deterioration of the spinal mechanical properties. Thus, the specimens of the current study were weaker than the population most likely to suffer whiplash trauma. To ensure that no specimen was prematurely injured due to excessive inertia loads from the surrogate head, we chose the 3.3 kg head mass. Using this head, the WCS + MFR model was developed and fine-tuned to produce an in vivo-like kinematic response during simulated whiplash experiments. Throughout the simulated whiplash, the surrogate head and WCS were completely stabilized with the compressive MFR forces, without requiring a tensile force to counterbalance the head weight. No head rest was used to restrict the head extension.

Coordinate systems The ground-fixed coordinate system (h–v) had h-axis oriented horizontally and v-axis vertically (Fig. 1a). The z–y system was parallel to the h–v system, but fixed to the sled.

Dynamic evaluation of the WCS + MFR model

To evaluate the dynamic performance of the WCS + MFR model, whiplash simulations were performed using a bench-top apparatus [59] and the incremental trauma protocol [2], at nominal T1 maximum horizontal accelerations of 3.5 g, 5 g, 6.5 g, and 8 g (Fig. 2). The main components of the bench-top whiplash apparatus included the sled to which the specimen was attached, impacting mass, power springs and braking system. The power springs were energized to a level specific for the desired maximum T1 horizontal acceleration. The impacting mass was released from the springs following a computer command, and it struck the sled from the rear. An accelerometer (part No. ADXL250JQC, Analog Devices, Norwood, MA, USA), oriented along the z-axis, was fixed to the sled to measure its acceleration. High-speed cameras (Kodak Motion Corder, Fast Cam, Super 10 k and model PS-110, Eastman Kodak, Rochester, NY, USA) recorded the sagittal plane motions of the vertebral and head flag markers at 500 frames/s.

Data analyses Custom Matlab programs were written to automatically track the motions of the flag markers throughout whiplash (Matlab, The Mathworks, Natick, MA, USA). The kinematic data were low-pass filtered at a cut-off frequency of 30 Hz and analyzed using Excel (Microsoft, Redmond, WA, USA). This frequency was determined through several preliminary trials, with the criterion of minimizing the vibration signals without losing the measured signal.

Results

Sled apparatus performance: T1 horizontal acceleration pulse

The average peak T1 horizontal accelerations measured during each of the whiplash simulations were within one standard deviation of the nominal input accelerations of 3.5 g, 5 g, 6.5 g, and 8 g (Table 2), demonstrating the accuracy of the computer-controlled bench-top whiplash apparatus. The average duration of the T1 horizontal acceleration was 103.6 ms (SD 9.2 ms), which compared favorably with ranges of 80 ms to 164 ms measured during real-life rear-end automobile collisions (Table 3).

WCS + MFR dynamic evaluation

A representative example Specimen No. 3, with measured T1 horizontal acceleration of 4.7 g, was chosen to illustrate the original high-speed movie images and the

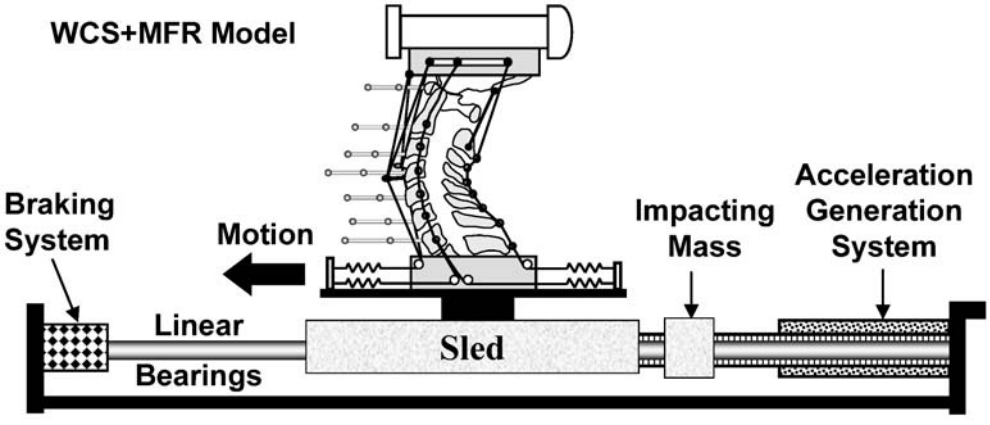

Fig. 2 Whiplash apparatus with the WCS + MFR model. The main components of the whiplash apparatus include the sled mounted on linear bearings, impacting mass, acceleration generation system consisting of power springs and a piston, and the braking system

Table 2 Average (SD) peak nominal T1 horizontal accelerations and measured accelerations (g) and velocities (kph) obtained during the simulated whiplash of the six specimens

Nominal peak T1 horizontal acceleration (g)	Measured peak T1 horizontal acceleration (g)	Measured peak T1 horizontal velocity (kph)
3.5	3.6 (0.1)	9.1 (0.1)
5	4.7 (0.3)	11.4 (0.2)
6.5	6.6 (0.2)	12.4 (0.3)
8	7.9 (0.3)	13.1 (0.3)

derived parameters (Fig. 3). The images shown are at: the onset of the T1 horizontal acceleration (0 ms), and 50 ms increments up to 250 ms (Fig. 3a). Initially, the head translated posteriorly ($-T_z$) approximately 0.8 cm without rotating (Fig. 3b). Then the head began rotating backwards ($-R_x$) and translating inferiorly ($-T_y$). The intervertebral rotations at the various levels varied with time (Fig. 3c). Note the S-shaped curvature from about 25 ms to 100 ms, defined by flexion at the upper levels (C0–C1, C1–C2 and C2–C3) and extension at the lower levels.

Anterior MFR cable loads The average (SD) peak force in the combined anterior MFR cables was 219.4 N (31.4 N), 243.0 N (19.2 N), 242.2 N (24.9 N), and 230.1 N (23.6 N) during the 3.5 g, 5 g, 6.5 g, and 8 g whiplash simulations, respectively. Thus, simulated whiplash caused increases in excess of 200 N in the intervertebral compressive pre-loads.

Head–T1 extension The average peak head–T1 extension of 37.1° during the 3.6 g peak acceleration (9.1 kph velocity) was within the in vivo corridor [16] that was established from rear-end impact volunteer tests at velocities between 7.6 kph and 9.3 kph (Table 4).

Intervertebral rotations The available data for in vivo rear-impact intervertebral rotation are limited. A single 4.6 g rear-end impact of one volunteer was reported by Kaneoka et al. [33] using 90 frames/second cineradiography, in which only the C2–C3 through C5–C6 rotations were recorded. The peak in vivo C4–C5 and C5–C6 intervertebral rotations were within the 95% confidence intervals of the average peak intervertebral rotations measured during the 4.7 g whiplash simulation of the current study. The peak in vivo intervertebral rotations at C2–C3 and C3–C4 marginally exceeded the 95% confidence intervals by 0.2° and 1.3°, respectively (Fig. 4).

Discussion

While the mechanisms that cause whiplash-associated disorders remain unknown, the facet joints have been identified by clinicians as a source of pain in whiplash patients [4, 5, 42, 43, 44]. Previous models used to study whiplash have included anthropometric test dummies [8, 17, 25, 40, 41, 71, 76, 77], mathematical models [12, 15, 16, 19, 20, 29, 39, 52, 87], whole cadavers [22, 23, 24, 25, 28, 45, 50, 89] and isolated whole cervical spine (WCS) specimens [13, 14, 26, 59, 60, 62, 74, 90]. These models either lack dynamic biofidelity or are not capable of providing insight into the facet joint and osteoligamentous injury mechanisms. Although the WCS model has several unique advantages, such as the measurement of all intervertebral motions during whiplash simulation and quantification of the functional injury, it does not replicate in vivo spinal loads or postural stability. The goals of the current study were to further develop the model by incorporating muscle force replication (MFR) [30, 63, 64], and then to evaluate the new model exper-

Table 3 Comparison of the average (SD) T1 horizontal acceleration pulse durations (ms) for the current study and the automobile acceleration pulse duration measured during real-life rear-end collisions. The number of impacts (*n*) and the measured peak accelerations (g) are also indicated

Reference	Acceleration duration (ms)	Peak acceleration (g)	*n*	Source of data
Current study	103.8 (11.0)	3.6 to 7.9	24	
Krafft et al. [36]	80.0 (32.4)	4.0 to 14.0	8	Crash pulse recorders of automobiles in rear-end collisions
Ono et al. [53]	100.0	2.5	1	Automotive rear-end collision
Geigl et al. [24]	110.0	3.1	1	Accident data recorder of automobiles in rear-end collisions
West et al. [85]	128.4 (19.7)	2.1 to 7.5	14	Human volunteer rear-end collision in various automobiles
Welcher et al. [84]	135.0 (21.2)	1.4 to 4.0	2	Cars in rear-end collisions (foam-to-foam-bumper interface)
Bailey [3]	140.0	3.2	1	Cars in rear-end collisions (foam-to-foam-bumper interface)
Severy et al. [73]	164.0 (41.0)	1.5 to 6.1	5	Pioneering study (cars with rigid bumpers)

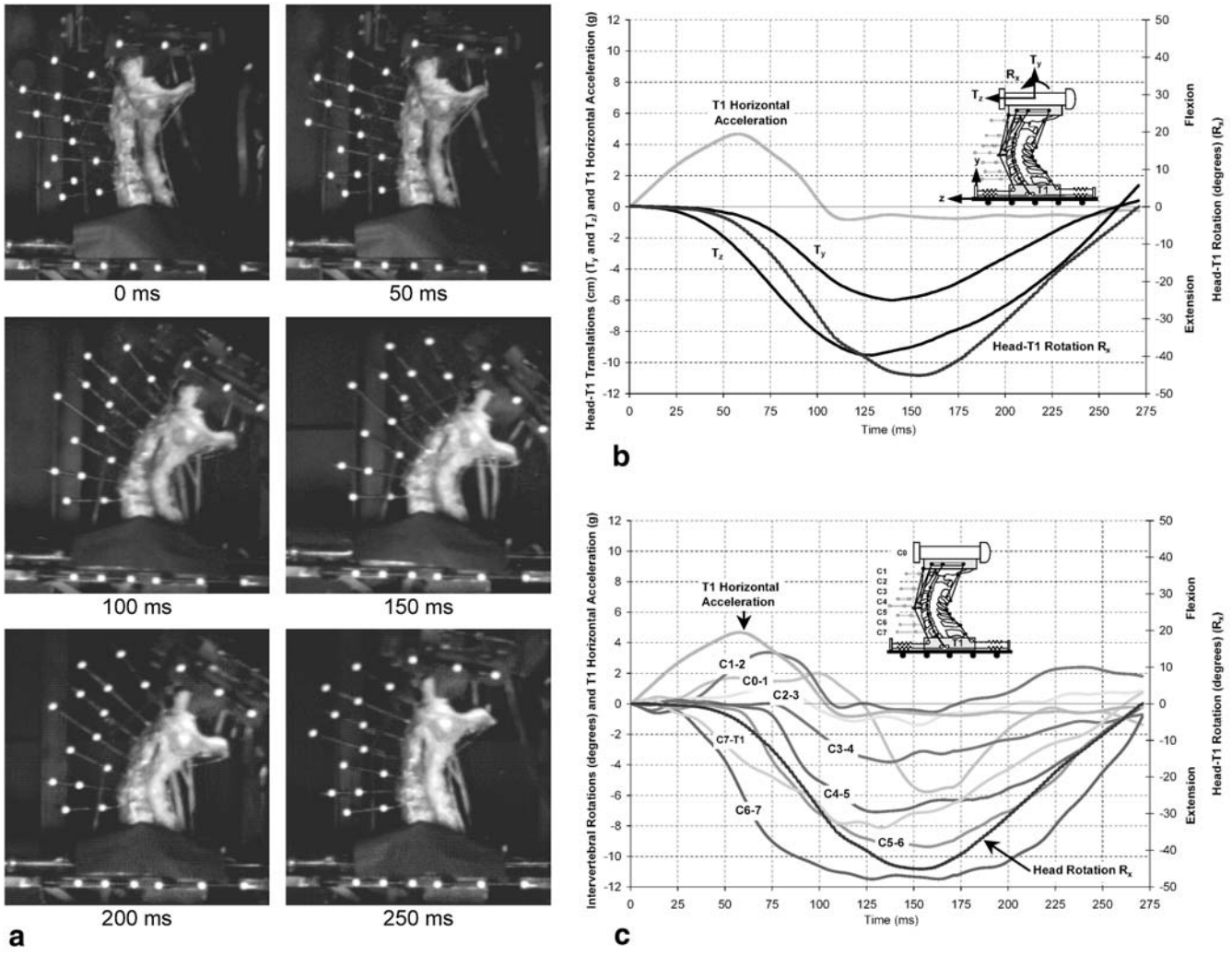

Fig. 3 A representative example of simulated whiplash (human specimen No. 3; peak T1 horizontal acceleration of 4.7 g). **a** High-speed digital camera images at times: 0 ms, 50 ms, 100 ms, 150 ms, 200 ms and 250 ms; **b** head displacements relative to T1: horizontal T_z and vertical T_y translations, and head rotation R_x in the sled coordinate system z–y, as functions of time; and **c** intervertebral rotations: C0–1 through C7–T1, head rotation R_x and T1 horizontal acceleration as functions of time

imentally by comparing the results with in vivo data. Our results served to validate the kinematic response of the new WCS + MFR model. The average peak head–T1 extension during the 9.1 kph impact was within the in vivo corridor [16], and within the ranges of previous in vivo studies that had not used head restraint (Table 4). The 95% confidence intervals of the average peak C4–C5 and C5–C6 intervertebral rotations of the WCS + MFR model encompassed the corresponding peak in vivo intervertebral rotations (Fig. 4) [33]. The peak in vivo intervertebral rotations at C2–C3 and C3–C4 of the young volunteer marginally exceeded the corresponding 95% upper confidence limits measured using the WCS + MFR model, most likely due to the higher age of the specimens of the current study.

The limitations of the WCS + MFR model include the fixation of the T1 vertebra to the sled, which may have affected the cervical spine kinematics, especially at C7–T1. Nonetheless, the kinematic response of the WCS + MFR model compared favorably with the corresponding in vivo data. The model did not attempt to replicate the innumerable intersegmental and global musculature or to model the active neuromuscular response. The MFR system provided neutral postural stability to the whole cervical spine specimen, via intervertebral compressive pre-loads that were in the range of values reported for volunteers in the relaxed posture [27, 51].

Recently, there have been several in vivo studies that have measured the electromyographic (EMG) signals from specific neck muscles during simulated whiplash.

Table 4 Average (with 95% confidence limits) peak head–T1 extension during the whiplash simulations of the current study and comparison with previous in vivo studies. The number of impacts (*n*) and the inclusion of a head rest are also indicated

Reference	*n*	Peak sled horizontal velocity (kph)	Peak head–T1 extension (degrees)	Head rest used?
Current study	6	9.1	37.1 (5.9)	No
		11.4	55.5 (14.8)	
		12.4	68.8 (15.4)	
		13.1	82.2 (12.9)	
Scott et al. [71]	3	3.9 to 7.8	15 to 40	Yes
Szabo et al. [78]	7	16	10 to 30	Yes
McConnell et al. [49]	3	7.7 to 9.2	45 to 57	Yes
Ono et al. [54]	3	2.2 to 4	39 to 50	No
Ono et al. [55]	17	4 to 8	25 to 50	No
Davidsson [17]	10	7.6 to 9.3	35 to 51	No
Welcher et al. [84]	15	4	7.5 to 27.4	Yes

Do the EMG signals indicate significant muscle forces to alter the course of neck injury development? We believe that this is not the case. For the muscle forces to alter the injury mechanisms, they need to develop immediately following the impact and be of sufficient magnitude. Ono et al. [55] performed rear-impact simulations using volunteers at peak velocity changes of 8 kph. They found that the average onset time of the neck flexors was 79 ms, and reported that an additional 70 to 100 ms was needed before peak muscle tension was achieved. They concluded that muscle tension did not alter head or neck kinematics if the neck muscles were relaxed prior to impact. Szabo et al. [78] performed a similar study at velocity changes up to 10 kph, and found that the initial muscle activity typically occurred 100 to 125 ms following impact, and that full muscle tension was not likely to develop for another 60 to 70 ms. Magnusson et al. [46] simulated rear impacts below 0.5 g and found that the average time to the onset of muscle activity was 112 ms, with additional time to reach peak muscle tension ranging between 43 ms and 184 ms. Kumar et al. [37] found that the sternocleidomastoid and trapezius reached peak activities at 162.9 ms and 923.9 ms, respectively, following a 1.4 g impact. Thus, since peak muscle tension occurs following the peak EMG activity, the earliest time to reach peak muscle tension was 149 ms. In the current study, the peak intervertebral extension occurred significantly earlier, 121 ms following the onset of the T1 horizontal acceleration. More importantly, extension of the lower cervical spine beyond the physiological limits may injure the cervical ligamentous components during the S-shaped phase of motion, prior to the peak intervertebral rotation [64]. Secondly, are the peak muscle forces of sufficient magnitude to alter the injury mechanism? Neck extension during whiplash can be restricted only by the neck flexor muscles. The peak flexion moment at C7–T1 produced by the cervical spine flexor muscles in healthy young volunteers during maximum voluntary neck flexion has ranged between 15 Nm and 30 Nm [32, 82]. During a simulated rear-impact with a peak T1 horizontal acceleration of 3.8 g, the peak extension moment at C7–T1 was found to exceed 30 Nm [59]. This implies that the muscles lack sufficient force to resist the inertial loads imposed on them during whiplash, even when the acceleration is below the injury threshold of 4.5 g [62]. Thus, we conclude that the neck muscle response time is not quick enough, and the neck muscle force is of insufficient magnitude, to alter the cervical spine kinematics during the injurious phase of whiplash.

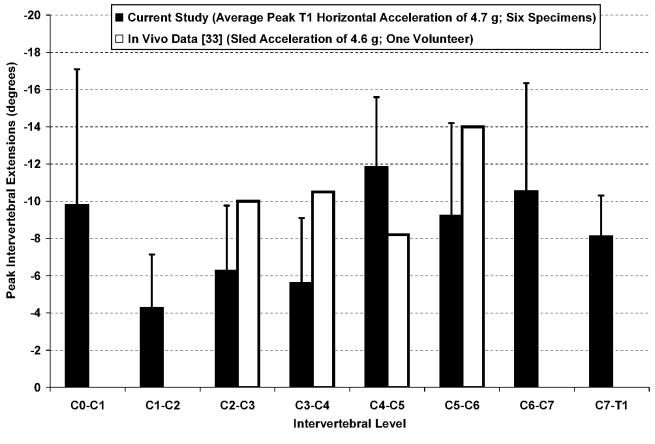

Fig. 4 Average (with 95% confidence limits) peak intervertebral rotations of the current study during average peak T1 horizontal acceleration of 4.7 g. Also shown are the available in vivo data from a cineradiographic study of a volunteer subjected to a simulated rear-end impact with peak sled acceleration of 4.6 g [33]

There exists potential for acute injury to the cervical spine musculature due to whiplash. The WCS + MFR model was not designed to evaluate these injuries. However, the chronic neck pain resulting from whiplash cannot be explained by muscle injury [72]. Since muscles have ample blood supply to promote healing, they are not likely to be the cause of chronic pain. In contrast,

whiplash-induced chronic symptoms may be explained by partial tears of the soft tissues, which do have poor blood supply. The annulus fibers and spinal ligaments contain mechanoreceptive and nociceptive nerve endings, and, when injured, they can cause chronic pain and clinical instability. In several clinical studies, facet-joint injuries have been demonstrated in whiplash patients [4, 5, 42, 43, 44]. The new WCS + MFR model is ideally suited to study these clinically important osteoligamentous injuries of the cervical spine.

Conclusions

In summary, a new in vitro WCS + MFR model for whiplash simulation has been developed and evaluated experimentally. The model behavior at low impact accelerations compared favorably to the data observed during whiplash simulation of volunteers. The peak head extension during the 3.6 g impact was within the in vivo corridor established using volunteers. The peak in vivo intervertebral rotations obtained during a 4.6 g whiplash simulation of a young volunteer were within, or only marginally in excess of, the 95% confidence limits of the average peak intervertebral rotations measured during the 4.7 g whiplash simulation of the WCS + MFR model. Having validated the dynamic biofidelity of the WCS + MFR model using volunteer data, we believe the model is capable of generating important biomechanical data that may help improve our understanding of whiplash injuries and injury mechanisms.

Acknowledgement This research was supported by NIH Grant 1 R01 AR45452 1A2.

References

1. Association for the Advancement of Automotive Medicine (1990) The abbreviated injury scale, 1990 revision. AAAM, Des Plaines, IL, USA
2. Atlas OK, Dodds SD, Panjabi MM (2002) Single and incremental trauma models: a biomechanical assessment of spinal instability. Eur Spine J 12:205–210
3. Bailey M (1996) Assessment of impact severity in minor motor vehicle collisions. Journal of Musculoskeletal Pain 4:21–38
4. Barnsley L, Lord S, Bogduk N (1993) Comparative local anaesthetic blocks in the diagnosis of cervical zygapophysial joint pain. Pain 55:99–106
5. Barnsley L, Lord SM, Wallis BJ, Bogduk N (1995) The prevalence of chronic cervical zygapophysial joint pain after whiplash. Spine 20:20–25
6. Becker EB (1972) Measurement of mass distribution parameters of anatomical segments. Society of Automotive Engineers Paper No. 720964
7. Bernhardt P, Wilke HJ, Wenger KH et al (1999) Multiple muscle force simulation in axial rotation of the cervical spine. Clin Biomech (Bristol, Avon) 14:32–40
8. Bostrom O, Fredriksson R, Haland Y et al (2000) Comparison of car seats in low speed rear-end impacts using the BioRID dummy and the new neck injury criterion (NIC). Accid Anal Prev 32:321–328
9. Braakman R, Penning L (1971) Injuries of the cervical spine. Excerpta Medica, Amsterdam
10. Brault JR, Siegmund GP, Wheeler JB (2000) Cervical muscle response during whiplash: evidence of a lengthening muscle contraction. Clin Biomech (Bristol, Avon) 15:426–435
11. Buonocore E, Hartman JT, Nelson CL (1966) Cineradiograms of cervical spine in diagnosis of soft-tissue injuries. JAMA 198:143–147
12. Camacho DL, Nightingale RW, Robinette JJ (1997) Experimental flexibility measurements for the development of a computational head-neck model validated for near-vertex head impact. Society of Automotive Engineers Paper No. 973345
13. Cholewicki J, Panjabi MM, Nibu K et al (1998) Head kinematics during in vitro whiplash simulation. Accid Anal Prev 30:469–479
14. Cusick JF, Pintar FA, Yoganandan N (2001) Whiplash syndrome: kinematic factors influencing pain patterns. Spine 26:1252–1258
15. Dauvilliers F, Bendjellal F, Weiss M (1994) Development of a finite element model of the neck. Society of Automotive Engineers Paper No. 942210
16. Davidsson J (2000) Development of a mechanical model for rear impacts: evaluation of volunteer responses and validation of the model. Dissertation, Chalmers University of Technology, Sweden
17. Davidsson J, Svensson M, Flogard A et al (1998) BioRID I—A new biofidelic rear impact dummy. International Research Council on the Biomechanics of Impacts. Goteborg, Sweden
18. Davis SJ, Teresi LM, Bradley WG Jr, Ziemba MA, Bloze AE (1991) Cervical spine hyperextension injuries: MR findings. Radiology 180:245–251
19. de Jager M (1996) Mathematical head-neck models for acceleration impacts. Dissertation, University of Eindhoven, The Netherlands
20. de Jager M, Sauren A, Thunnissen J, Wismans J (1996) A global and a detailed mathematical model for head-neck dynamics. Society of Automotive Engineers Paper No. 962430
21. Dvorak J, Panjabi MM, Novotny JE, Antinnes JA (1991) In vivo flexion/extension of the normal cervical spine. J Orthop Res 9:828–834
22. Eichberger A, Darok M, Steffan H et al (2000) Pressure measurements in the spinal canal of post-mortem human subjects during rear-end impact and correlation of results to the neck injury criterion. Accid Anal Prev 32:251–260
23. Fast A, Sosner J, Begeman P, Thomas MA, Chiu T (2002) Lumbar spinal strains associated with whiplash injury: a cadaveric study. Am J Phys Med Rehabil 81:645–650
24. Geigl BC, Steffan H, Leinzinger P et al (1994) The movement of the head and cervical spine during rear-end impact. International Research Conference on the Biomechanics of Impacts. Lyon, France

25. Geigl BC, Steffan H, Leinzinger P et al (1995) Comparison of head-neck kinematics during rear end impact between standard hybrid III, RID neck, volunteers and PMTO's. International Conference on the Biomechanics of Impacts. Brunnen, Switzerland
26. Grauer JN, Panjabi MM, Cholewicki J, Nibu K, Dvorak J (1997) Whiplash produces an S-shaped curvature of the neck with hyperextension at lower levels. Spine 22:2489–2494
27. Hattori S, Oda H, Kawai S (1981) Cervical intradiscal pressure in movements and traction of the cervical spine. Z Orthop 119:568–569
28. Hodgson VR, Thomas LM (1980) Mechanisms of cervical spine injury during impact to the protected head. 24th STAPP Car Crash Conference, Society of Automotive Engineers. Warrendale, PA, USA
29. Horst M (2002) Human head neck response in frontal, lateral and rear end impact loading: modelling and validation Dissertation, Eindhoven University of Technology, The Netherlands
30. Ivancic PC, Pearson AM, Panjabi MM, Ito S (2004) Injury of the anterior longitudinal ligament during whiplash simulation. Eur Spine J 13:61–68
31. Jonsson H Jr, Bring G, Rauschning W, Sahlstedt B (1991) Hidden cervical spine injuries in traffic accident victims with skull fractures. J Spinal Disord 4:251–263
32. Jordan A, Mehlsen J, Bulow PM, Ostergaard K, Danneskiold-Samsoe B (1999) Maximal isometric strength of the cervical musculature in 100 healthy volunteers. Spine 24:1343–1348
33. Kaneoka K, Ono K, Inami S, Yokoi N, Hayashi K (1997) Human cervical spine kinematics during whiplash loading. International Conference on New Frontiers in Biomechanical Engineering. Tokyo, Japan
34. Kaneoka K, Ono K, Inami S, Hayashi K (1999) Motion analysis of cervical vertebrae during whiplash loading. Spine 24:763–769
35. Kettler A, Hartwig E, Schultheiss M, Claes L, Wilke HJ (2002) Mechanically simulated muscle forces strongly stabilize intact and injured upper cervical spine specimens. J Biomech 35:339–346
36. Krafft M, Kullgren A, Tingvall C, Bostrom O, Fredriksson R (2000) How crash severity in rear impacts influences short- and long-term consequences to the neck. Accid Anal Prev 32:187–195
37. Kumar S, Narayan Y, Amell T (2002) An electromyographic study of low-velocity rear-end impacts. Spine 27:1044–1055
38. Lind B, Sihlbom H, Nordwall A, Malchau H (1989) Normal range of motion of the cervical spine. Arch Phys Med Rehabil 70:692–695
39. Linder A (2000) A new mathematical neck model for a low-velocity rear-end impact dummy: evaluation of components influencing head kinematics. Accid Anal Prev 32:261–269
40. Linder A, Bergman U, Svensson M, Viano D (2000) Evaluation of the Bio-RID P3 and the Hybrid III in pendulum impacts to the back—a comparison to human subject test data. Annu Proc Assoc Adv Automot Med 44:283–297
41. Linder A, Olsson T, Truedsson N et al (2001) Dynamic performances of different seat designs for low to medium velocity rear impact. Annu Proc Assoc Adv Automot Med 45:187–201
42. Lord SM, Barnsley L, Bogduk N (1995) Percutaneous radiofrequency neurotomy in the treatment of cervical zygapophysial joint pain: a caution. Neurosurgery 36:732–739
43. Lord SM, Barnsley L, Wallis BJ, Bogduk N (1996) Chronic cervical zygapophysial joint pain after whiplash. A placebo-controlled prevalence study. Spine 21:1737–1744
44. Lord SM, Barnsley L, Wallis BJ, McDonald GJ, Bogduk N (1996) Percutaneous radio-frequency neurotomy for chronic cervical zygapophyseal-joint pain. N Engl J Med 335:1721–1726
45. Luan F, Yang KH, Deng B et al (2000) Qualitative analysis of neck kinematics during low-speed rear-end impact. Clin Biomech (Bristol, Avon) 15:649–657
46. Magnusson ML, Pope MH, Hasselquist L et al (1999) Cervical electromyographic activity during low-speed rear impact. Eur Spine J 8:118–125
47. Matsushita T, Sato TB, Hirabayashi K et al (1994) X-ray study of the human neck motion due to head inertia loading. Society of Automotive Engineers Paper No. 942208. 1994
48. McConnell WE, Howard RP, Guzman HM et al (1993) Analysis of human test subject kinematic responses to low velocity rear end impacts. Society of Automotive Engineers Paper No. 930889
49. McConnell WE, Howard RP, Poppel JV et al (1995) Human head and neck kinematics after low velocity rear-end impacts—understanding "whiplash." Society of Automotive Engineers Paper No. 952724
50. Mertz HJ, Patrick LM (1971) Strength and response of the human neck. Society of Automotive Engineers Paper 710855. Warrendale, PA
51. Moroney SP, Schultz AB, Miller JA (1988) Analysis and measurement of neck loads. J Orthop Res 6:713–720
52. Nitsche S, Krabbel G, Appel H (1996) Validation of a finite element model of the human neck. International Conference on the Biomechanics of Impacts
53. Ono K, Kanno M (1993) Influences of the physical parameters on the risk of neck injuries in low impact speed rear-end collisions. International Conference on the Biomechanics of Impacts. Eindhoven, The Netherlands
54. Ono K, Kanno M (1996) Influences of the physical parameters on the risk to neck injuries in low impact speed rear-end collisions. Accid Anal Prev 28:493–499
55. Ono K, Kaneoka K, Wittek A, Kajzer J (1997) Cervical injury mechanism based on the analysis of human cervical vertebral motion and head-neck-torso kinematics during low speed rear impacts. Society of Automotive Engineers Paper No. 973340
56. Ordway NR, Seymour RJ, Donelson RG, Hojnowski LS, Edwards WT (1999) Cervical flexion, extension, protrusion, and retraction. A radiographic segmental analysis. Spine 24:240–247
57. Panjabi M (1979) Validation of mathematical models. J Biomech 12:238
58. Panjabi MM (1998) Cervical spine models for biomechanical research. Spine 23:2684–2700
59. Panjabi MM, Cholewicki J, Nibu K, Babat LB, Dvorak J (1998) Simulation of whiplash trauma using whole cervical spine specimens. Spine 23:17–24
60. Panjabi MM, Cholewicki J, Nibu K et al (1998) Mechanism of whiplash injury. Clin Biomech (Bristol, Avon) 13:239–249
61. Panjabi MM, Crisco JJ 3rd, Lydon C, Dvorak J (1998) The mechanical properties of human alar and transverse ligaments at slow and fast extension rates. Clin Biomech (Bristol, Avon) 13:112–120
62. Panjabi MM, Nibu K, Cholewicki J (1998) Whiplash injuries and the potential for mechanical instability. Eur Spine J 7:484–492
63. Panjabi MM, Miura T, Cripton PA et al (2001) Development of a system for in vitro neck muscle force replication in whole cervical spine experiments. Spine 26:2214–2219
64. Panjabi MM, Pearson AM, Ito S, Ivancic PC, Wang JL (2004) Cervical spine curvature during simulated whiplash. Clin Biomech (Bristol Avon) 19:1–9
65. Patwardhan AG, Havey RM, Meade KP, Lee B, Dunlap B (1999) A follower load increases the load-carrying capacity of the lumbar spine in compression. Spine 24:1003–1009

66. Patwardhan AG, Havey RM, Ghanayem AJ et al (2000) Load-carrying capacity of the human cervical spine in compression is increased under a follower load. Spine 25:1548–1554
67. Quint U, Wilke HJ, Loer F, Claes L (1998) Laminectomy and functional impairment of the lumbar spine: the importance of muscle forces in flexible and rigid instrumented stabilization—a biomechanical study in vitro. Eur Spine J 7:229–238
68. Quint U, Wilke HJ, Shirazi-Adl A et al (1998) Importance of the intersegmental trunk muscles for the stability of the lumbar spine. A biomechanical study in vitro. Spine 23:1937–1945
69. Richter M, Otte D, Pohlemann T, Krettek C, Blauth M (2000) Whiplash-type neck distortion in restrained car drivers: frequency, causes and long-term results. Eur Spine J 9:109–117
70. Rohlmann A, Neller S, Claes L, Bergmann G, Wilke HJ (2001) Influence of a follower load on intradiscal pressure and intersegmental rotation of the lumbar spine. Spine 26:E557–E561
71. Scott MW, McConnell WE, Guzman HM et al (1993) Comparison of human and ATD head kinematics during low-speed rear-end impacts. Society of Automotive Engineers Paper No. 930094
72. Scott S, Sanderson PL (2002) Whiplash: a biochemical study of muscle injury. Eur Spine J 11:389–392
73. Severy DM, Mattewson JH, Bechtol CO (1955) Controlled automobile rear-end collisions, an investigation of related engineering and medical phenomena. Can Serv Med J 11:727–759
74. Stemper BD, Yoganandan N, Pintar FA (2002) Intervertebral rotations as a function of rear impact loading. Biomed Sci Instrum 38:227–231
75. Sturzenegger M, Radanov BP, Di Stefano G (1995) The effect of accident mechanisms and initial findings on the long-term course of whiplash injury. J Neurol 242:443–449
76. Svensson MY, Lovsund P, Haland Y, Larsson S (1993) The influence of seatback and head-restraint properties on the head-neck motion during rear-impact. International Research Conference on the Biomechanics of Impacts. Eindhoven, The Netherlands
77. Svensson MY, Bostrom O, Davidsson J et al (2000) Neck injuries in car collisions—a review covering a possible injury mechanism and the development of a new rear-impact dummy. Accid Anal Prev 32:167–175
78. Szabo TJ, Welcher JB (1996) Human subject kinematics and electromyographic activity during low speed rear impacts. Society of Automotive Engineers Paper No. 962432
79. Szabo TJ, Welcher JB, Anderson RD et al (1994) Human occupant kinematic response to low speed rear-end impacts. Society of Automotive Engineers Paper No. 940532
80. Taylor JR, Twomey LT (1993) Acute injuries to cervical joints. An autopsy study of neck sprain. Spine 18:1115–1122
81. Uhrenholt L, Grunnet-Nilsson N, Hartvigsen J (2002) Cervical spine lesions after road traffic accidents: a systematic review. Spine 27:1934–1941
82. Vasavada AN, Li S, Delp SL (2001) Three-dimensional isometric strength of neck muscles in humans. Spine 26:1904–1909
83. Walker LB, Harris EH, Pontius UR (1973) Mass, volume, center of mass, and mass moment of inertia of head and neck of human body. Society of Automotive Engineers Paper No. 730985
84. Welcher JB, Szabo TJ (2001) Relationships between seat properties and human subject kinematics in rear impact tests. Accid Anal Prev 33:289–304
85. West DH, Gough JP, Harper GTK (1993) Low speed rear-end collision testing using human subjects. Accident Reconstruction Journal:22–26
86. Wilke HJ, Wolf S, Claes LE, Arand M, Wiesend A (1995) Stability increase of the lumbar spine with different muscle groups. A biomechanical in vitro study. Spine 20:192–198
87. Yang KY, Zhu F, Luan F (1998) Development of a finite element model of the human neck. Society of Automotive Engineers Paper No. 983157
88. Yoganandan N, Pintar F, Butler J et al (1989) Dynamic response of human cervical spine ligaments. Spine 14:1102–1110
89. Yoganandan N, Cusick JF, Pintar FA, Rao RD (2001) Whiplash injury determination with conventional spine imaging and cryomicrotomy. Spine 26:2443–2448
90. Yoganandan N, Pintar FA, Cusick JF (2002) Biomechanical analyses of whiplash injuries using an experimental model. Accid Anal Prev 34:663–671